

Tuning magnetization in Ni-Fe-Gd thin films by using the electrodeposition technique

P. Sathishkumar^{1,*}, E. Elayaperumal¹, S.G. Juliana², D. Azhakanantham³, A.A. Ghfar⁴, and A. Ganguly³

¹Department of Physics, Sri Paramakalyani College, Alwarkurichi-627412, Tamil Nadu, India

²Department of Physics, Nazareth Margoschis College, Nazareth-628 617, Tamil Nadu, India

³Department of Physics & Nanotechnology, SRM Institute of Science & Technology, Kattankulathur-603203, Tamil Nadu, India

⁴Department of Chemistry, College of Science, King Saud University, P.O. Box 2455, Riyadh-11451, Saudi Arabia

*Corresponding author e-mail: perumal_sathish@yahoo.co.in

Abstract. Thin films with soft magnetic properties are critical for advanced magnetic data storage and transfer devices. This study focuses on the electrodeposition of Ni-Fe-Gd thin film alloys onto copper substrates, varying current densities to investigate their structural, compositional, morphological, and magnetic properties. The obtained films display complex crystalline structures comprising mixed face-centered cubic (FCC), body-centered cubic (BCC), and hexagonal close-packed (HCP) phases depending on the Gd ion content and deposition conditions. The observed magnetic behavior ranges from superparamagnetic to soft ferromagnetic, depending on the Gd interaction with Ni and Fe and local microstructural defects. This study is significant in advancing the development of magnetic alloy-based thin films for magnonic and spintronic applications.

Keywords: ferromagnetism, electrodeposition, magnetic properties, Ni-Fe-Gd thin films.

<https://doi.org/10.15407/spqeo28.02.166>

PACS 75.60.Ej, 81.15.Pq, 82.45.Qr

Manuscript received 24.12.24; revised version received 31.03.25; accepted for publication 11.06.25; published online 26.06.25.

1. Introduction

Magnetic nanostructures made from iron group metals (Fe, Co, and Ni) and their alloys have drawn significant attention due to their high saturation magnetization, low magnetostriction, small coercive field, and well-optimized magnetic anisotropy [1, 2]. More importantly, these thin film alloys are in high demand due to their tunable and customizable properties, making them ideal for various applications [3–8]. The Ni-Fe alloys with 10–90% iron are one of the most versatile soft magnetic alloys, which have been used as inductor cores in microelectronics [9], magnetic recording heads (Ni₈₀Fe₂₀ and Ni₄₅Fe₅₅) [10], magnetic sensors [11–14], energy harvesters [15, 16], tunable noise suppressor [17], and magnetic actuators and motors [18]. Anisotropic magneto-resistance properties are observed in the magnetic alloys relevant for spintronic applications [19–21]. The constituent elements and their Ni-Fe structure determine their magnetoresistive characteristics [3]. The Ni₃₆Fe₆₄ alloys have been utilized in large-size cryogenic liquid containers and high-definition color displays [22]. The advantage of tunable magnetic properties is the ability to drive various magnetic phenomena used in spintronics and biomedicine. Examples include magnetic bubbles

[23] and domain walls-based memory devices [24], magnetic imaging [25], targeted drug delivery [26] and cancer therapy [27].

In the last few decades, rare earth (RE) – transition metal (TM) alloys have attracted the attention of the research community due to their rich magnetic phase diagram with complex types of magnetic ordering [28]. Generally, in transition metals, the 3d electrons occupy the outer shells and are delocalized and subjected to strong direct exchange interactions. In rare earth metals, the 4f electrons are localized and subjected to indirect exchange interactions mediated by 5d and 6s electrons, resulting in high magnetic moments per atom. A ferromagnetic coupling that occurs in TM with light RE elements leads to increase in magnetization, whereas ferrimagnetic coupling occurs in TM with heavy RE elements, resulting in a decrease in magnetization. The occurrence of antiferromagnetic coupling between TM and RE has been explained by Campbell *et al.* [29]. The interactions between 3d electrons of Ni, Fe, Co and 5d electrons of Gd are negative because the d band in TM is more than half-filled, whereas in RE it is less than half-filled. Thus, the antiferromagnetic coupling of spins is observed due to the combination of 4f-5d and 5d-3d interactions.

Owing to the enormous number of unpaired electrons, RE ions afford high magnetic moments in a magnetic field [30]. The ions of RE metals have a superior magnetic moment and magneto-crystalline anisotropy, which distinguishes them from 3d transition metals. However, the ions of rare earth metals enhance the concentration of vacancies and magnetic properties, decreasing the leakage current [31]. Due to the high perpendicular magnetic anisotropy and large magnetostriction, the Gd-based ferromagnetic alloys have potential applications in magneto-optical storage recording, bubble memories and advanced dichroic coherent imaging [32–34]. The RE-TM alloy thin films are found to be a good candidate for use in the field of ultrafast magnetization dynamics due to the antiferromagnetic coupling between the Gd and Fe sub-lattices [35]. Hence, by making a material which combines these three (Fe, Gd, Ni) metals, one can obtain interesting magnetic behaviour, useful for magnonic device applications. The early studies on yttrium iron garnets also show that the addition of RE elements can enhance the dynamic damping [36, 37]. Although numerous studies have been carried out to investigate the magnetic properties of binary TM-RE thin films, namely Fe-Gd, Co-Gd, Ni-Gd and so on, with a focus on the effect of RE on TM. It is worth noting that the Ni-Fe-Gd (ternary TM-RE) thin films have not yet been electrodeposited.

Electrodeposition is the simplest method for the metals and alloys thin films formation onto conductive substrates. The deposited thin films are formed in a stable crystalline phase or thermodynamically metastable phase, which can be transformed into a more stable phase by heat treatment [38]. Electrodeposition methods for the preparation of magnetic thin films have several advantages, namely simple equipment, ease of operation, low cost and so on. The properties of deposited alloys depend strongly on the experimental parameters, namely bath composition, potential, pH, temperature and applied current [39, 40]. During the electrodeposition process, pH and current density are two key variables that determine the physical properties of the deposited films [41, 42].

In this study, we comprehensively examine how the elemental composition, structure, morphology, and magnetic properties of the electrodeposited Ni-Fe-Gd (TM-RE) thin films are influenced by the current density used during the electrodeposition of these films. Additionally, we explore the impact of Gd on the magnetic characteristics of Ni-Fe-Gd soft magnetic thin films.

2. Experimental detail

2.1. Thin film preparation process

The deposition bath comprised 0.1 M of NiCl₂ and FeCl₂ and 0.01M of GdCl₃·6H₂O, 1 g of boric acid (H₃BO₃) and 1 g of citric acid (C₆H₈O₇·H₂O). All the raw chemicals are of analytical reagent grade. A Cu substrate of size 1.5×5 cm was cut out from a commercially available copper foil with a thickness of 0.1 mm used as a cathode, and the same size of pure steel as an anode (counter electrode) for electrodeposition experiments.

The substrate surface was carefully cleaned with sandpaper and then covered with adhesive tape except for the area on which the deposition of films was desired. All samples were pre-treated as follows: soak the substrate and counter electrode in distilled water for 3 min at room temperature, purification by 5% H₂SO₄ for 5 min, and rinse with distilled water for 3 min just before deposition. To fabricate Ni-Fe-Gd thin films, the electrodeposition process was carried out on copper substrates applying three current densities of 13, 27 and 40 mA·cm⁻² and the corresponding currents of 100, 200 and 300 mA, respectively, at room temperature without stirring for 30 min. Boric acid and citric acid were used to enhance the electrodeposition of nickel and iron. The pH of the electrolyte was adjusted to 5 by using a few drops of ammonia solution.

2.2. Characterization

The fabricated thin films were examined for their structural, morphological and magnetic properties. The thickness of Ni-Fe-Gd thin films electrodeposited at various current densities has been measured using the Stylus profilometer, SurfTest SJ-301. The structural properties of the films were investigated using XRD with CuK_α radiation ($\lambda = 1.5405 \text{ \AA}$). The surface morphology of nanostructured thin films was scrutinized using a Quanta 200FEG scanning electron microscope (SEM). The magnetic properties of electrodeposited thin films were measured at room temperature using a vibrating sample magnetometer (VSM) model VSM Lakeshore-7400.

3. Results and discussion

3.1. XRD study

The crystalline structure of Ni-Fe-Gd films deposited at pH = 5 applying current densities of 13, 27 and 40 mA·cm⁻² on the Cu substrates was investigated using XRD within the range 5°...90° as shown in Fig. 1. The XRD pattern of Ni_{46.45}Fe_{49.14}Gd_{4.40} film deposited at 13 mA·cm⁻² shows diffraction peaks at 38.32° and 77.9° attributed to (111) and (220) planes of Cu substrate and the peaks at 44.56° and 77.9° attributed to (111) and (220) plane of FCC structure of NiFe according to the JCPDS-PDF-004-0850. The closed peaks at 64.86° and 65.08° represent the reflections from (200) and (004) planes of the BCC structure of Fe and Gd, respectively, shown in the inset of Fig. 1 [43]. It is worth noting that the mixed FCC/BCC phase of Ni-Fe-Gd alloys is obtained by electrodeposition applying a current density of 13 mA·cm⁻². With increasing the current density to 27 and 40 mA·cm⁻², the reflections from Fe(200) (64.86°) and Gd(004)(65.08°) disappear completely in both Ni_{37.86}Fe_{56.81}Gd_{5.32} and Ni_{12.03}Fe_{69.94}Gd_{18.03} films. The increase of Gd contents leads to the formation of additional crystalline phases [44]. It is found that the disappearance of the Cu (111) peak at 38.32° is caused by the shielding effect of the thicker NiFeGd film on the substrate with increasing current density. It is also observed that the peaks at 44.56° and 77.9° attributed to NiFe (111) and NiFe (220)/Cu (220) planes are shifted

toward lower angles (43.8° and 74.1°) with increasing current density.

Moreover, the increase of Gd content with current density induces a new diffraction peak at 50.44° attributed to the HCP (110) plane of Gd in the XRD patterns of both films. The latter can be explained by the formation of a new sublattice with mixed FCC/HCP phases in the NiFe structure. The XRD study revealed that the deposited Ni-Fe-Gd films are crystalline, containing mixed FCC/BCC and FCC/HCP phases depending on the Gd content and applied current density. The average crystallite size of the electrodeposited Ni-Fe-Gd films was calculated from the full width at half maximum of the NiFe(111) peak using the Scherrer formula [45]. The obtained sizes are 65.36, 61.08, and 54.54 nm for the current densities of 13, 27, and $40 \text{ mA}\cdot\text{cm}^{-2}$, respectively, as given in the table. It is found that the average crystallite size decreases with increasing current density.

3.2. Morphological study

To observe the microstructure and composition of Ni-Fe-Gd thin films, SEM imaging and EDX measurements are carried out. Usually, higher current density causes a large grain size [40,48], and increases the thickness of the coated films, but in the presence of various mixtures of metal precursors, the effect of current density can differ and the change in morphology and composition is not always straightforward relation [46]. Fig. 2 shows the SEM and EDX images of the surface of Ni-Fe-Gd thin films electrodeposited from a chloride bath at room temperature with current densities of 13, 27, and $40 \text{ mA}\cdot\text{cm}^{-2}$. One can see that when the current density of $13 \text{ mA}\cdot\text{cm}^{-2}$, the Ni-Fe-Gd film has an almost equal amount of Ni (46.45 wt.%) and Fe (49.14 wt.%) contents with Gd (04.40 wt.%), more agglomerations are formed in samples, which may be due to the magnetic ion interaction between Ni and Fe in the presence of Gd as shown in Fig. 2a. With increasing current density, the surface of the Ni-Fe-Gd film has a grain-like morphology, smooth and uniform, without any crack as shown in Fig. 2b. The latter can be explained by the decreased Ni content in the film ($46.45 \rightarrow 37.86 \text{ wt.}\%$) and the increased iron content ($49.14 \rightarrow 56.81 \text{ wt.}\%$) with increasing Gd content. The mechanism that determines the size of grains is the following. The increase of Gd content with current density may inhibit grain growth by pinning grain boundaries, preventing the formation of large grains and promoting a finer grain structure. This finer grain structure can contribute to a smoother and more uniform surface. The increase of Gd content may also reduce internal stresses within the thin film by accommodating mismatched lattices. This stress relaxation mechanism helps to prevent crack formation and maintain a uniform surface. It is also observed that at $40 \text{ mA}\cdot\text{cm}^{-2}$, white circular regions with granular shapes are developed on the surface of the sample, which indicates the increased Fe content, while dark base regions – the decreased Ni content, as shown in Fig. 2c [47]. Another work demonstrates the formation of nodular structures and coarser

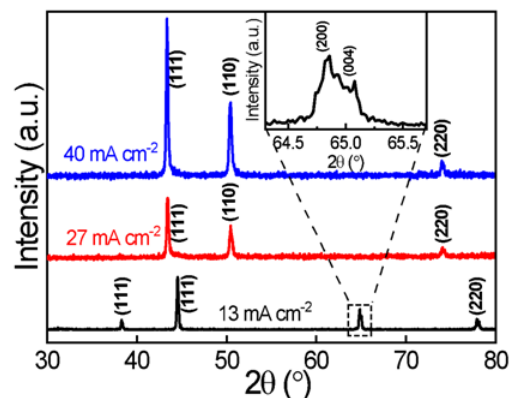


Fig. 1. XRD patterns of electrodeposited Ni-Fe-Gd thin films for the current densities of 13, 27, and $40 \text{ mA}\cdot\text{cm}^{-2}$, respectively.

grains with increasing the current density [48]. Therefore, this surface modification in the Ni-Fe-Gd film is caused by the complex effect of precursor concentration and metallic ions interaction, influenced by the current density.

3.3. Elemental composition

The changes in the elemental composition of electrodeposited thin films are caused by the following factors: concentration of ions, pH, temperature and applied current, which leads to changes in the crystalline structure and grain size of electrodeposited layers [49, 50]. Here, the effect of current density on film composition was analyzed in the case of fixed (30 min) deposition time. The measured thicknesses of Ni-Fe-Gd thin films for current densities of 13, 27, and $40 \text{ mA}\cdot\text{cm}^{-2}$ are 12.32, 15.41, and $17.46 \mu\text{m}$, respectively. If the electrolytic potential of Fe is more favorable under the given conditions, an increase in current density may improve the deposition of Fe onto electrode surfaces. Conversely, Ni has the ability to deteriorate the deposition due to a less favorable electrolytic potential at higher current densities [48]. Our results show that the efficiency of Gd embedding in the deposited films increases linearly with increasing current density, whereas the efficiency of Ni and Fe embedding varies nonlinearly with current density. Particularly, the Ni content decreases with increasing current density while the Fe content increases and *vice versa* as shown in Fig. 3a. This nonlinear variation of Ni and Fe contents with current density is due to the following mechanism: the anomalous co-deposition can either be enhanced or suppressed by adjusting the electrodeposition parameters [5]. For the co-deposition of Ni and Fe atoms, the Fe component is controlled by activation, whereas the Ni component is controlled by diffusion [51]. Since the cathodic overpotential increases with increasing cathodic current density, it leads to an increase in the nucleation rate [48]. This overpotential causes an increase in Fe content and consequently a decrease in the Ni content of deposited Ni-Fe-Gd thin films [52]. However, the total deposition rate still increases with the applied current density.

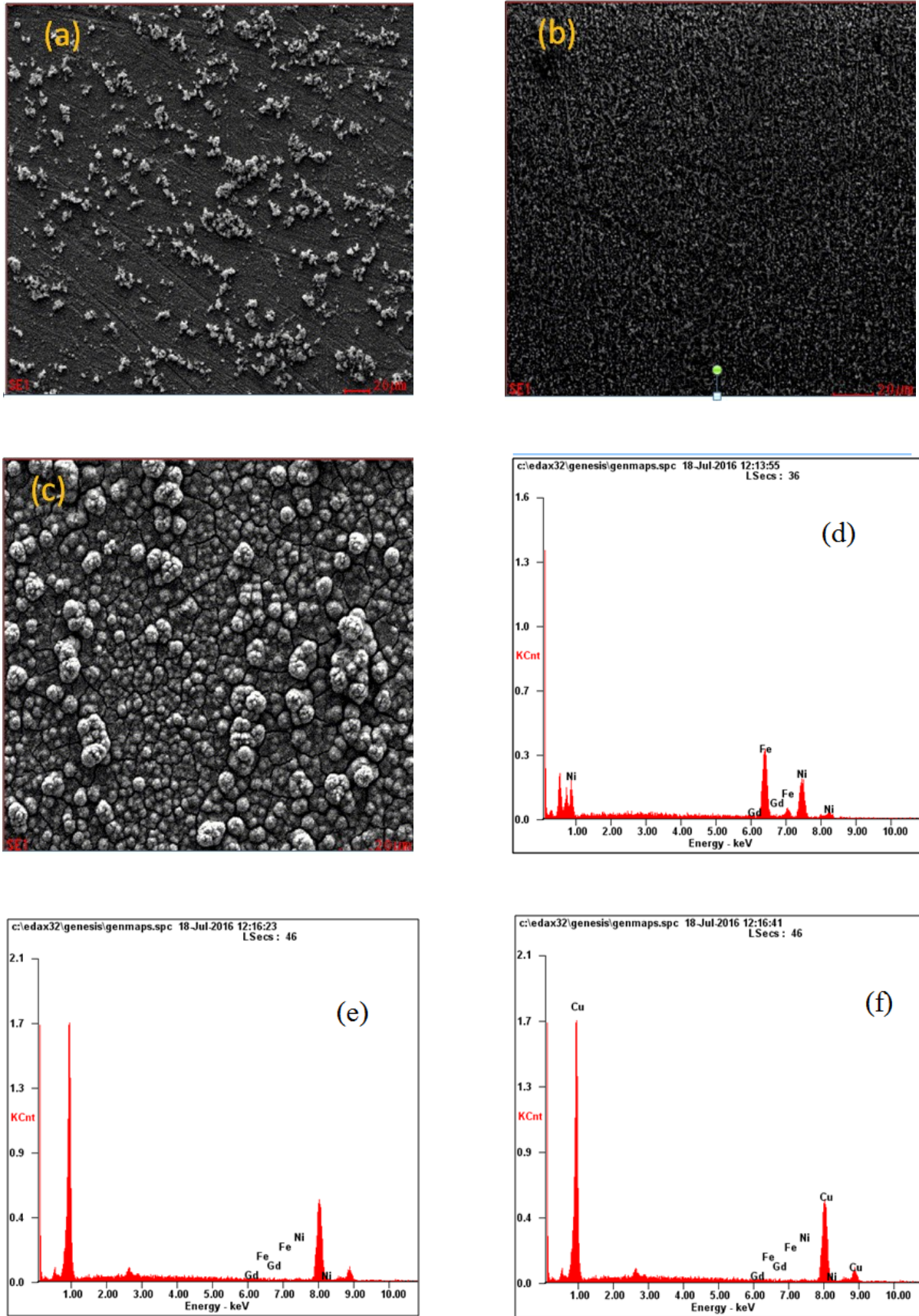


Fig. 2. SEM micrographs and EDX spectra of the electrodeposited Ni-Fe-Gd thin films with current densities of 13 (a, d), 27 (b, e), and 40 mA·cm⁻² (c, f), respectively.

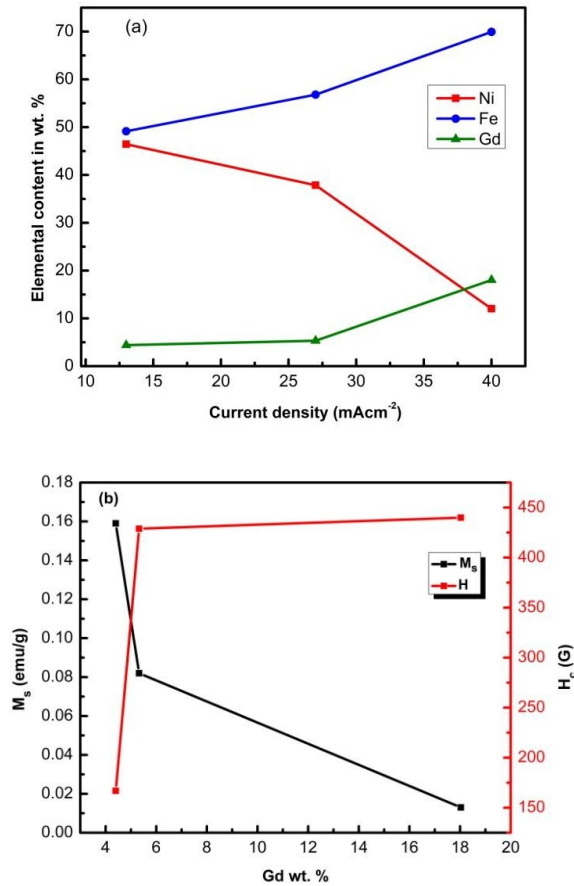


Fig. 3. The variation of elemental contents in wt.% depending on the current density (a) and M_s and H_c value as a function of Gd contents in Ni-Fe-Gd thin films (b).

3.4. Magnetic properties

Fig. 4 shows the hysteresis loops for the Ni-Fe-Gd thin films deposited on a copper substrate at a pH of 5 and current densities of 13, 27, and 40 mA·cm⁻². Table summarizes the values of remanent magnetization (M_r), coercivity (H_c), and saturation magnetization (M_s) for these films. The relationship between M_s and H_c values and Gd content is illustrated in Fig. 3b. One can see a linear variation, represented by the black line in the hysteresis loop diagram, in Fig. 4. This line, which passes very close to the origin, exhibits a steep slope typical of ferromagnets, with minimal coercivity and remanence.

This behavior indicates superparamagnetism, where individual magnetic domains act like single, non-interacting particles, aligning with an external magnetic field but not retaining magnetization once the field is removed [53]. The specific Gd concentration in the Ni-Fe alloy influences its microstructure, promoting superparamagnetic-like behavior. However, the curve does not exhibit saturation, likely because saturation occurs at a higher field beyond the measurement range. The enhanced M_s can be attributed to several factors: Gd high magnetic anisotropy may increase the overall anisotropy of the alloy, raising the saturation field. Gd could also

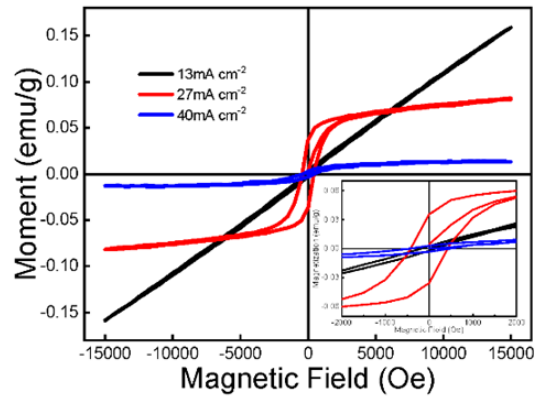


Fig. 4. Hysteresis loops of the electrodeposited Ni-Fe-Gd thin films for the current densities of 13, 27 and 40 mA·cm⁻², respectively.

improve exchange coupling between Fe and Ni atoms, leading to stronger cooperative magnetic behavior, requiring a higher external field for saturation. Gd may also stabilize magnetic phases with higher coercivity and saturation fields compared to the pure Fe-Ni system.

In the second case, as the current density increases to 27 mA·cm⁻², the remanent magnetization (M_r) and coercivity (H_c) of the Ni_{37.86}Fe_{56.81}Gd_{5.32} alloy increase, indicating a transition from superparamagnetic to soft ferromagnetic behavior [54, 55]. This suggests that the higher current density during the electrodeposition enhances the crystallinity of the Ni-Fe-Gd thin film, which in turn promotes high ferromagnetic ordering. The improved crystallinity leads to better alignment of crystal grains and magnetic domains, resulting in increased magnetic coupling and stability. Thus, the rise in current density acts as a driving force, transitioning the material from superparamagnetism to soft ferromagnetism by promoting a higher magnetic order within the alloy. Finally, at the current density of 40 mA·cm⁻², the electrodeposited Ni_{12.03}Fe_{69.94}Gd_{18.03} thin film shows a weakening of the hysteresis loop signal (magnetic moment) with a saturation moment of 0.013 emu/g. Despite this reduction, the loop still demonstrates distinct soft magnetic behavior, with remanent magnetization (M_r) and coercivity (H_c) values of approximately 2.69 m·emu/g and 439.91 G, respectively.

Our findings align with previously reported results for (Ni₈₃Fe₁₇)_{1-x}Gd_x thin films, where the saturation magnetization decreases with increasing Gd content [56]. In our experiment, we observe that the room temperature saturation magnetization decreases almost linearly with increasing Gd content, which is consistent with the antiparallel alignment of Gd atomic moments relative to the Ni-Fe moment. This is illustrated in Fig. 3b. On the other hand, the coercivity (H_c) of magnetic materials is influenced by the particle size and magnetocrystalline anisotropy. The electrodeposition current and corresponding Gd concentration play a crucial role in determining the alloy properties as well as the grain size of the film.

Table. The parameters obtained from compositional, structural and magnetic measurements.

S. No	J (mA·cm ⁻²)	EDX			XRD			VSM		
		Ni (wt.%)	Fe (wt.%)	Gd (wt.%)	Peak position (degree)	FWHM (degree)	Grain size (nm)	Ms (emu/g)	Mr (emu/g)	Hc (Oe)
1	13	46.45	49.14	04.40	44.56	0.22923	65.36	> 0.159	0.0025	166.90
2	27	37.86	56.81	05.32	43.36	0.24427	61.08	0.082	0.0358	428.90
3	40	12.03	69.94	18.03	43.44	0.27362	54.54	0.013	0.0027	439.91

A reduction in the grain size can lead to smaller magnetic domains, resulting in higher Hc values [40]. In our study, the coercivity (Hc) increases with both current density and higher Gd content, reaching its maximum at the highest Gd concentration (18.03 wt.%). From the morphological analysis of the sample, it is found that increasing Gd concentration reduces the crystal size, which is in line with the observed increase of coercivity. In this study, the ability to finely tune the hysteretic properties of Ni-Fe-Gd thin films using electrodeposition conditions provides significant versatility, making them suitable for a wide range of applications in advanced magnonic and spintronic devices.

4. Conclusions

In conclusion, Ni-Fe-Gd thin film alloys with three distinct compositions were electrodeposited on copper substrates with varying current densities under constant pH conditions. X-ray diffraction revealed that the films possess high crystallinity with mixed FCC/BCC and FCC/HCP phases, free of impurity phases. As the current density is increased, a reduction in crystalline size is observed. SEM analysis showed diverse surface morphologies, ranging from particle agglomerations to grain-like and granular structures. EDX results indicated a linear increase in Gd content with current density, while Ni and Fe contents varied nonlinearly. VSM analysis demonstrated a superparamagnetic behavior at lower Gd concentrations, with a transition to soft ferromagnetism as Gd concentration increased. The saturation magnetization decreased nearly linearly with higher Gd content due to the antiparallel alignment of Gd atomic moments with the NiFe matrix. Coercivity (Hc) increases with decreasing grain size. These findings suggest that Ni-Fe-Gd thin films hold great potential for applications in magnonic and spintronic devices due to their tunable magnetic properties.

Acknowledgment

The authors are grateful to the Researchers Supporting Project Number (RSP2024R407), King Saud University, Riyadh, Saudi Arabia, for the financial support, and research funding from SRM Institute of Science and Technology, India (SRMIST/R/AR(A)/SERI2024/174/41/342) for the financial support.

References

- Mahato B.K., Ganguly A., Rana B., Barman A. Magnetization reversal in chemically synthesized hexagonal cobalt microplatelets. *J. Phys. Chem. C*. 2012. **116**. P. 22057–22062. <https://doi.org/10.1021/jp307144j>.
- Rana B., Ganguly A., Barman A. Magnetic shape anisotropy in chemically synthesized chains of nickel nanoparticles. *IEEE Trans. Magn.* 2011. **47**. P. 2859–2862. <https://doi.org/10.1109/TMAG.2011.2140364>.
- Zubar T.I., Fedosyuk V.M., Trukhanov A.V. *et al.* Control of growth mechanism of electrodeposited nanocrystalline NiFe films. *J. Electrochem. Soc.* 2019. **166**. P. D173–D180. <https://doi.org/10.1149/2.1001904jes>.
- Hjiri M., Alshammari S., Besbes H. *et al.* The effect of Ni/Fe ratio on the physical properties of NiFe₂O₄ nanocomposites. *Mater. Res. Express*. 2019. **6**. P. 086107. <https://doi.org/10.1088/2053-1591/ab201c>.
- Zubar T.I., Sharko S.A., Tishkevich D.I. *et al.* Anomalies in Ni-Fe nanogranular films growth. *J. Alloys Compd.* 2018. **748**. P. 970–978. <https://doi.org/10.1016/j.jallcom.2018.03.245>.
- Torabinejad V., Aliofkhaeaei M., Assareh S. *et al.* Electrodeposition of Ni-Fe alloys, composites, and nano coatings – A review. *J. Alloys Compd.* 2017. **691**. P. 841–859. <https://doi.org/10.1016/j.jallcom.2016.08.329>.
- Torabinejad V., Rouhaghdam A.S., Aliofkhaeaei M., Allahyarzadeh M.H. Electrodeposition of Ni-Fe and Ni-Fe-(nano Al₂O₃) multilayer coatings. *J. Alloys Compd.* 2016. **657**. P. 526–536. <https://doi.org/10.1016/j.jallcom.2015.10.154>.
- Béland L.K., Samolyuk G.D., Stoller R.E. Differences in the accumulation of ion-beam damage in Ni and NiFe explained by atomistic simulations. *J. Alloys Compd.* 2016. **662**. P. 415–420. <https://doi.org/10.1016/j.jallcom.2015.11.185>.
- Kubo E., Ooi N., Aoki H. *et al.* Effect of magnetic field on permeability of electroplated permalloy for microdevices. *Jpn. J. Appl. Phys.* 2010. **49**. P. 04DB17. <https://doi.org/10.1143/JJAP.49.04DB17>.
- Koo B., Yoo B. Electrodeposition of low-stress NiFe thin films from a highly acidic electrolyte. *Surf. Coat. Tech.* 2010. **205**. P. 740–744. <https://doi.org/10.1016/j.surfcoat.2010.07.076>.

11. Sun N.X., Srinivasan G. Voltage control of magnetism in multiferroic heterostructures and devices. *SPIN*. 2012. **02**. P. 1240004. <https://doi.org/10.1142/S2010324712400048>.
12. Grabchikov S.S., Trukhanov A.V., Trukhanov S.V. *et al.* Effectiveness of the magnetostatic shielding by the cylindrical shells. *J. Magn. Magn. Mater.* 2016. **398**. P. 49–53. <https://doi.org/10.1016/j.jmmm.2015.08.122>.
13. Kondalkara V.V., Lia X., Yanga S., Leea K. Current sensor based on nanocrystalline NiFe/Cu/NiFe thin film. *Procedia Eng.* 2016. **168**. P. 675–679. <https://doi.org/10.1016/j.proeng.2016.11.245>.
14. Trukhanov A.V., Grabchikov S.S., Solobai A.A. *et al.* AC and DC-shielding properties for the Ni₈₀Fe₂₀/Cu film structures. *J. Magn. Magn. Mater.* 2017. **443**. P. 142–148. <https://doi.org/10.1016/j.jmmm.2017.07.053>.
15. Phuoc N.N., Xu F., Ong C.K. Ultrawideband microwave noise filter: Hybrid antiferromagnet/ferromagnet exchange-coupled multilayers. *Appl. Phys. Lett.* 2009. **94**. P. 092505. <https://doi.org/10.1063/1.3094881>.
16. Jiraskova Y., Bursik J., Turek I. *et al.* Phase and magnetic studies of the high-energy alloyed Ni–Fe. *J. Alloys Compd.* 2014. **594**. P. 133–140. <https://doi.org/10.1016/j.jallcom.2014.01.138>.
17. Gardner D.S., Schrom G., Hazucha P. *et al.* Integrated on-chip inductors using magnetic material (invited). *J. Appl. Phys.* 2008. **103**. P. 07E927. <https://doi.org/10.1063/1.2838012>.
18. Tseng Y.-T., Wu G.-X., Lin J.-C. *et al.* Preparation of Co-Fe-Ni alloy micropillar by microanodeguided electroplating. *J. Alloys Compd.* 2021. **885**. P. 160873. <https://doi.org/10.1016/j.jallcom.2021.160873>.
19. Myung N.V., Nobe K. Electrodeposited iron group thin-film alloys: Structure-property relationships. *J. Electrochem. Soc.* 2001. **148**. P. C136. <https://doi.org/10.1149/1.1345875>.
20. Ganguly A., Kondou K., Sukegawa H. *et al.* Thickness dependence of spin torque ferromagnetic resonance in Co₇₅Fe₂₅/Pt bilayer films. *Appl. Phys. Lett.* 2014. **104**. P. 072405. <https://doi.org/10.1063/1.4865425>.
21. Mondal S., Choudhury S., Jha N. *et al.* All-optical detection of the spin Hall angle in W/CoFeB/SiO₂ heterostructures with varying thickness of the tungsten layer. *Phys. Rev. B.* 2017. **96**. P. 054414. <https://doi.org/10.1103/PhysRevB.96.054414>.
22. Pepperhoff W., Acet M. *Constitution and Magnetism of Iron and Its Alloys*. Springer, Berlin, Heidelberg, 2001. <https://doi.org/10.1007/978-3-662-04345-5>.
23. Ganguly A., Zhang S., Miron I.M. *et al.* Competition between chiral energy and chiral damping in the asymmetric expansion of magnetic bubbles. *ACS Appl. Electron. Mater.* 2021. **3**. P. 4734–4742. <https://doi.org/10.1021/acsaelm.1c00592>.
24. Barman S., Ganguly A., Barman A. Configuration and polarization dependent transverse domain wall motion and domain wall switching in ferromagnetic nanowire. *SPIN*. 2013. **03**. P. 1350001. <https://doi.org/10.1142/S201032471350001X>.
25. Zhang S., Zhang X., Zhang J. *et al.* Direct imaging of an inhomogeneous electric current distribution using the trajectory of magnetic half-skyrmions. *Sci. Adv.* 2020. **6**. P. eaay1876. <https://doi.org/10.1126/sciadv.aay1876>.
26. Guo S., Li D., Zhang L. *et al.* Monodisperse mesoporous superparamagnetic single-crystal magnetite nanoparticles for drug delivery. *Biomaterials*. 2009. **30**. P. 1881–1889. <https://doi.org/10.1016/j.biomaterials.2008.12.042>.
27. Maity D., Chandrasekharan P., Pradhan P. *et al.* Novel synthesis of superparamagnetic magnetite nanoclusters for biomedical applications. *J. Mater. Chem.* 2011. **21**. P. 14717. <https://doi.org/10.1039/c1jm11982f>.
28. Camley R.E., Stamps R.L. Magnetic multilayers: spin configurations, excitations and giant magnetoresistance. *J. Phys.: Condens. Matter.* 1993. **5**. P. 3727–3786. <https://doi.org/10.1088/0953-8984/5/23/003>.
29. Campbell I.A. Indirect exchange for rare earths in metals. *J. Phys. F: Met. Phys.* 1972. **2**. P. L47–L50. <https://doi.org/10.1088/0305-4608/2/3/004>.
30. Suresh R., Sathishkumar P., Kumaravelan S., Seshadri S. Magnetic properties and microstructure of Co–Ni–Fe–Gd–Mn electrodeposited thin film. *Surf. Rev. Lett.* 2021. **28**. P. 2050039. <https://doi.org/10.1142/S0218625X20500390>.
31. Suresh R., Sathishkumar P., Kumaravelan S. *et al.* Soft magnetic properties of Co–Ni–Fe–Gd/Cu electrodeposited thin film. *J. Mater. Sci.: Mater. Electron.* 2020. **31**. P. 18037–18044. <https://doi.org/10.1007/s10854-020-04354-y>.
32. Meiklejohn W.H. Magneto-optics: A thermomagnetic recording technology. *Proc. IEEE*. 1986. **74**. P. 1570–1581. <https://doi.org/10.1109/PROC.1986.13669>.
33. Hansen P., Clausen C., Much G. *et al.* Magnetic and magneto-optical properties of rare-earth transition-metal alloys containing Gd, Tb, Fe, Co. *J. Appl. Phys.* 1989. **66**. P. 756–767. <https://doi.org/10.1063/1.343551>.
34. Umadevi K., Talapatra A., Chelvane J.A. *et al.* Magnetic anisotropy and microscopy studies in magnetostrictive Tb-(Fe,Co) thin films. *J. Appl. Phys.* 2017. **122**. P. 065108. <https://doi.org/10.1063/1.4998451>.
35. Radu I., Stamm C., Eschenlohr A. *et al.* Ultrafast and distinct spin dynamics in magnetic alloys. *SPIN*. 2015. **05**. P. 1550004. <https://doi.org/10.1142/S2010324715500046>.
36. Spencer E.G., LeCraw R.C., Clogston A.M. Low-temperature line-width maximum in yttrium iron garnet. *Phys. Rev. Lett.* 1959. **3**. P. 32–33. <https://doi.org/10.1103/PhysRevLett.3.32>.
37. Sirvetz M.H., Zneimer J.E. Microwave properties of polycrystalline rare earth garnets. *J. Appl. Phys.* 1958. **29**. P. 431–433. <https://doi.org/10.1063/1.1723169>.

38. Watanabe T. *Nano-plating: Microstructure Control Theory of Plated Film and Data Base of Plated Film Microstructure*. Elsevier, 2004.
39. Perez L., Attenborough K., De Boeck J. *et al.* Magnetic properties of CoNiFe alloys electrodeposited under potential and current control conditions. *J. Magn. Magn. Mater.* 2002. **242–245**. P. 163–165. [https://doi.org/10.1016/S0304-8853\(01\)01190-8](https://doi.org/10.1016/S0304-8853(01)01190-8).
40. Min J.H., Wu J.-H., Cho J.U. *et al.* The pH and current density dependence of DC electrodeposited CoCu thin films. *J. Magn. Magn. Mater.* 2006. **304**. P. e100–e102. <https://doi.org/10.1016/j.jmmm.2006.01.191>.
41. Boubatra M., Azizi A., Schmerber G., Dinia A. The influence of pH electrolyte on the electrochemical deposition and properties of nickel thin films. *Ionics*. 2012. **18**. P. 425–432. <https://doi.org/10.1007/s11581-011-0642-3>.
42. Pandit B., Goda E.S., Shaikh S.F. Electrochemical Deposition Toward Thin Films, in: B.R. Sankapal, A. Ennaoui, R.B. Gupta, C.D. Lokhande (Eds.), *Simple Chemical Methods for Thin Film Deposition: Synthesis and Applications*. Springer Nature, Singapore, 2023. P. 245–304. https://doi.org/10.1007/978-981-99-0961-2_6.
43. Tabakovic I., Inturi V., Thurn J., Kief M. Properties of $\text{Ni}_{1-x}\text{Fe}_x$ ($0.1 < x < 0.9$) and Invar ($x = 0.64$) alloys obtained by electrodeposition. *Electrochim. Acta*. 2010. **55**. P. 6749–6754. <https://doi.org/10.1016/j.electacta.2010.05.095>.
44. Schmidt N.Y., Abdulazhanov S., Michalička J. *et al.* Effect of Gd addition on the structural and magnetic properties of $L1(0)$ -FePt alloy thin films. *J. Appl. Phys.* 2022. **132**. P. 213908. <https://doi.org/10.1063/5.0124652>.
45. Gorria P., Martínez-Blanco D., Pérez M.J. *et al.* Structure and magnetism of Fe-rich nanostructured Fe–Ni metastable solid solutions. *J. Magn. Magn. Mater.* 2005. **294**. P. 159–164. <https://doi.org/10.1016/j.jmmm.2005.03.030>.
46. Liao Y., Gabe D.R., Wilcox G.D. Microstructural Morphology of Zn-Fe Alloy Electrodeposited Coatings. *Plating and Surface Finishing*. 1998. P. 62–66.
47. Hacıismailoglu M., Alper M. Effect of electrolyte pH and Cu concentration on microstructure of electrodeposited Ni–Cu alloy films. *Surf. Coat. Technol.* 2011. **206**. P. 1430–1438. <https://doi.org/10.1016/j.surfcoat.2011.09.010>.
48. Zhang Y.L., Wang Q., Wang D.T. *et al.* Effect of current density, reaction temperature and deposition time on the electrodeposition of ZrB_2 coating. *J. Mater. Eng. Perform.* 2024. **34**. P. 1016–1025. <https://doi.org/10.1007/s11665-023-09115-6>.
49. Liu C.-M., Tseng Y.-C., Chen C. *et al.* Superparamagnetic and ferromagnetic Ni nanorod arrays fabricated on Si substrates using electroless deposition. *Nanotechnology*. 2009. **20**. P. 415703. <https://doi.org/10.1088/0957-4484/20/41/415703>.
50. Sarac U., Baykul M.C. Effect of applied current density on morphological and structural properties of electrodeposited Fe–Cu films. *J. Mater. Sci. Technol.* 2012. **28**. P. 1004–1009. [https://doi.org/10.1016/S1005-0302\(12\)60165-0](https://doi.org/10.1016/S1005-0302(12)60165-0).
51. Su C., Zhao L., Tian L. *et al.* Rapid electrodeposition of Fe–Ni alloy foils from chloride baths containing trivalent iron ions. *Coatings*. 2019. **9**. P. 56. <https://doi.org/10.3390/coatings9010056>.
52. Yang C.-C., Shu M.-F. Preparation of perpendicular GdFeCo magnetic thin films with pulse electrodeposition technique utilizing molten salt as electrolyte. *Z. Naturforsch. A*. 2007. **62**. P. 761–768. <https://doi.org/10.1515/zna-2007-1215>.
53. Zhang Y., Liu M., Zhang Y. *et al.* Atomic layer deposition of superparamagnetic and ferrimagnetic magnetite thin films. *J. Appl. Phys.* 2015. **117**. P. 17C743. <https://doi.org/10.1063/1.4916818>.
54. Drovosekov A.B., Kreines N.M., Savitsky A.O. *et al.* Magnetization and ferromagnetic resonance in a Fe/Gd multilayer: experiment and modelling. *J. Phys.: Condens. Matter*. 2017. **29**. P. 115802. <https://doi.org/10.1088/1361-648X/aa54f1>.
55. Cherifi K., Dufour C., Marchal G. *et al.* Magnetic structure of Gd/Fe multilayers. *J. Magn. Magn. Mater.* 1992. **104–107**. P. 1833–1834. [https://doi.org/10.1016/0304-8853\(92\)91569-F](https://doi.org/10.1016/0304-8853(92)91569-F).
56. Fu Y., Sun L., Wang J.S. *et al.* Magnetic properties of $(\text{Ni}_{83}\text{Fe}_{17})_{1-x}\text{Gd}_x$ thin films with diluted Gd doping. *IEEE Trans. Magn.* 2009. **45**. P. 4004–4007. <https://doi.org/10.1109/TMAG.2009.2024164>.

Authors and CV



P. Sathishkumar, Assistant Professor at the Sri Paramakalyani College, Tamil Nadu, India since 2017. He defended his PhD thesis in Theoretical Physics in Materials Science in 2011 at the Periyar University, Salem, Tamil Nadu, India. Authored over 26 publications. The area of his scientific interests includes nonlinear dynamics in magnetic materials, thin films and nanoparticles. <http://orcid.org/0000-0002-8607-9295>



E. Elayaperumal, Assistant Professor at the Sri Paramakalyani College, Tamil Nadu, India since 2017. He defended his PhD thesis in Physics (Materials Science) in 2016 at VIT University, Vellore, India. Authored 5 publications. The area of his research interest includes multiferroic materials, ferroelectric ceramics.

E-mail: eeppsk@gmail.com,
<https://orcid.org/0000-0001-9542-9827>



Dheebanthan Azhakanantham, Research Scholar in department of Physics and Nanotechnology, SRM Institute of Science and Technology. He is currently pursuing his Ph.D. in the Department of Physics with a focus on solar cells and perovskite semiconductors. He has over 9 peer-reviewed publications in reputed journals with impact factors ranging from 2.8 to 5.5. His research areas include nanotechnology, solar cell (especially perovskite-based photovoltaics), and thin-film semiconductor.

E-mail: deebanflamo@gmail.com,
<https://orcid.org/0009-0001-8062-0474>



Ayman Abdel GhfarHamed Ahmed, Assistant Professor at the Faculty in Chemistry Department, College of Science, King Saud University. His research interest is fabrication of novel clay-nano-composites (Green-Echo friendly nano-materials) for purification of industrial waste water, municipal waste water and drinking water. Fabrication of Novel Stainless Steel Chromatographic Column packed with “Clay-nano-composite” for Nano-HPLC applications. He has over 177 peer-reviewed publications in reputed journals with an H-index of 38. E-mail: aghafra@ksu.edu.sa,
<http://orcid.org/0000-0002-6685-7918>

industrial waste water, municipal waste water and drinking water. Fabrication of Novel Stainless Steel Chromatographic Column packed with “Clay-nano-composite” for Nano-HPLC applications. He has over 177 peer-reviewed publications in reputed journals with an H-index of 38. E-mail: aghafra@ksu.edu.sa,
<http://orcid.org/0000-0002-6685-7918>



S. Gracelin Juliana, defended her Ph.D. thesis in Physics (Materials Science) at the Manonmaniam Sundaranar University, India, in 2019. She is the Assistant Professor at the Department of Physics, Nazareth Margoschis College, India. Authored over 10 publications. The area of her scientific interests includes crystal growth and nanocomposites.

E-mail: juliana@nmcp.ac.in



Arnab Ganguly, Research Assistant Professor at SRM Institute of Science and Technology, India, since 2024. Earlier, he performed as a research scientist at Khalifa University, UAE, and a post-doctoral fellow at KAUST, Saudi Arabia. Dr. Ganguly received his Ph.D. from S.N. Bose National Centre for Basic Sciences, India, in 2016. Authored 19 publications. Dr. Ganguly is an accomplished material scientist who specialises in experimental as well as simulation studies of micro-/nano-structured materials. He investigates the spintronic, magnetic, and plasmonic properties of metallic multilayer thin films and artificial nanocrystals for sensor and data storage applications.

Centre for Basic Sciences, India, in 2016. Authored 19 publications. Dr. Ganguly is an accomplished material scientist who specialises in experimental as well as simulation studies of micro-/nano-structured materials. He investigates the spintronic, magnetic, and plasmonic properties of metallic multilayer thin films and artificial nanocrystals for sensor and data storage applications.

E-mail: arnabg@srmist.edu.in,
<https://orcid.org/0000-0001-9483-2227>

Authors' contributions

Sathishkumar P.: formal analysis, project administration and supervision, writing – review & editing.

Elayaperumal E.: writing – original draft, visualization, conceptualization, methodology, resources, data curation.

Gracelin Juliana S.: material preparation, data curation.

Azhakanantham D.: visualization, conceptualization.

Ghfar A.A.: resources, data curation, writing – review & editing.

Ganguly A.: formal analysis, investigation, data curation.

Регулювання намагніченості у тонких плівках Ni-Fe-Gd методом електроосадження

P. Sathishkumar, E. Elayaperumal, S.G. Juliana, D. Azhakanantham, A.A. Ghfar, and A. Ganguly

Анотація. Тонкі плівки з м'якими магнітними властивостями є критично важливими для магнітних пристроїв зберігання та передачі даних. Дане дослідження сфокусовано на електроосадженні тонкоплівкових сплавів Ni-Fe-Gd на мідних підкладках при варіюванні густини струму для вивчення їх складу, структурних, морфологічних та магнітних властивостей. Отримані плівки демонструють комплексні кристалічні структури, що включають змішані гранецентровану кубічну (ГЦК), об'ємно-центровану кубічну (БЦК) та гексагональну щільноупаковану (ГПУ) фази, в залежності від вмісту іонів Gd та умов осадження. Спостережувана магнітна поведінка варіюється від суперпарамагнітної до м'якої феромагнітної, в залежності від взаємодії Gd з Ni та Fe, а також локальних мікроструктурних дефектів. Таке дослідження є важливим для розвитку тонких плівок на основі магнітних сплавів для магнітних та спінтронних застосувань.

Ключові слова: феромагнетизм, електроосадження, магнітні властивості, тонкі плівки Ni-Fe-Gd.